ELSEVIER

Polymer 40 (1999) 3743–3752

polymer

The crystallization behavior of blends of thermotropic liquid crystalline polymers

M.A. McLeod, D.G. Baird*

Department of Chemical Engineering and the Center for Composite Materials and Structures, Virginia Polytechnic Institute and State University, Blacksburg, VA 24061-0211, USA

Received 14 April 1998; received in revised form 31 July 1998; accepted 9 August 1998

Abstract

This work was concerned with how the crystallization temperature of a thermotropic liquid crystalline polymer (TLCP) was lowered when blended with a second TLCP, with both TLCPs believed to be composed of various ratios of terephthalic acid, 4-hydroxybenzoic acid (HBA), hydroquinone, and hydroquinone derivatives. Specifically, HX6000, with a melting temperature of 332°C, was melt blended with HX8000, with a melting temperature of 272°C. Measuring the complex viscosities of the melt blends as they were cooled showed that a linear relationship between composition and solidification temperature existed. Studying the blends using differential scanning calorimetry (DSC) demonstrated that the crystallization temperature was lowered by addition of HX8000, as well as by using faster cooling rates. Dynamic mechanical analysis revealed that the storage and loss moduli decreased with the addition of HX8000 and the moduli declined sharply at lower temperatures relative to neat HX6000. Additional testing was performed to help understand this behavior, with the results suggesting that the TLCPs reacted with one another when the test samples were injection molded.

Keywords: Thermotropic liquid crystalline polymer; Polymer blends; Crystallization

1. Introduction

Thermotropic liquid crystalline polymers (TLCPs) have gained increased commercial attention because of their unique properties. These include their low coefficients of thermal expansion, low viscosity, high modulus, low permeability to gases, low dielectric constants, and chemical resistance [1–5]. As the demand for these characteristics increases, it is anticipated that the use of TLCPs will grow, rising at a projected annual growth rate of 25% from an estimated use of 10 million pounds per year in 1996 [2].

In expanding the potential uses for TLCPs, it has been found that TLCP/TLCP blends can possess characteristics which are better than those of either individual TLCP [6–13]. One improved characteristic that some TLCP/TLCP blends possess is a viscosity lower than either of the neat resins, making them easier to melt process [9–13]. For example, Isayev and Ding [9] melt blended Vectra A950, a copolyester containing 73 mol% 4-hydroxybenzoic acid (HBA) and 27 mol% 2-hydroxy-6-naphthoic acid (HNA), with Ultrax KR4003, a TLCP believed to contain *p*-oxybenzoyl, terephthaloyl, and hydroquinone moieties. They found that at a composition of 25/75 wt% Vectra A950/Ultrax KR4003, the blend had a viscosity lower than either of the neat resins. They speculated that this was due to slippage between the Vectra A950/Ultrax KR4003 interface and/or slippage at the TLCP/capillary wall interface. A second advantage that has been reported is that some TLCP/TLCP blends have mechanical properties which are higher than either neat resin [7–9,13]. For example, Kenig and colleagues [13] injection molded test specimens of a blend of two TLCPs, which they designated as copolymer A and copolymer B. Copolymer A contained 73 mol% HBA and 27 mol% HNA, while copolymer B contained 60 mol% HNA, 20 mol% terephthalic acid (TA), and 20 mol% acetoxy-acid aniline. They found that at a composition of 25 wt% copolymer A and 75 wt% copolymer B, the tensile strength was 343 MPa and the tensile modulus was 22.8 GPa. This was greater than the strength and modulus of either copolymer which were 244 MPa and 13.1 GPa, respectively, for copolymer A and 291 MPa and 21.4 GPa, respectively, for copolymer B. Hence, in some cases, creating TLCP/TLCP blends has produced key improvements in material behavior compared with either of the neat resins.

* Corresponding author. Tel.: +1-540-231-5998; Fax: +1-540-231-5022; E-mail: dbaird@vt.edu

0032-3861/99/$ - see front matter
PII: S0032-3861(98)00592-8

Because of the importance of melt viscosity in polymer processing operations, the complex viscosity of TLCP/TLCP blends has been measured as the melt was cooled to monitor solidification behavior. Baird and coworkers [6,14] studied copolyesters of HBA and poly(ethylene terephthalate) (PET), melt blending HBA/PET 60/40 mol% pellets with 80/20 mol% pellets at various weight fractions, then cooling the molten samples while measuring the complex viscosity. They found that solidification could be tailored to a specific temperature between the two extremes of the neat materials by simply adjusting the weight fractions of the two components.

In addition to the rheological test results, differential scanning calorimetry (DSC) has been used to monitor the crystallization of HBA/HNA copolyester blends and HBA/PET copolyester blends as they were cooled. De Meuse and Jaffe [11] ran cooling scans on blends of copolyesters of HBA/HNA and showed a single crystallization exotherm, from which they suggested that co-crystallization between the two TLCPs had occurred. McCullagh and colleagues [15] melt blended 75/25 mol% copoly(HBA/NNA) with 30/70 mol% copoly(HBA/HNA) to produce an overall monomer mole ratio of 60/40 HBA/HNA. They found that immediately after blending a compatible blend was formed, but that melt transesterification between the two components occurred as well. Ramanathan and coworkers [6] also ran DSC cooling scans on blends of copolyesters of HBA/PET to complement rheological cooling scans and found that the solidification temperatures obtained from the rheological tests were considerably higher than the temperatures determined from the DSC tests. However, the cooling rates for the rheological tests were not well controlled and did not match the 10°C/min rate used in the calorimeter, so direct comparisons between the two sets of data were not possible.

The purpose of this paper is to further explore the concept of modifying the crystallization behavior of a TLCP by blending it with a second TLCP of lower melting point. In conjunction with this focus, the effect of cooling rate on the crystallization temperature is examined and a possible reason explaining why this behavior exists is presented. It should be noted that the practical significance of this work rests in tailoring the solidification of TLCPs, thereby enhancing the ability to combine them with thermoplastics possessing lower processing temperatures [16–22].

2. Experimental

2.1. Materials

Two TLCPs produced by DuPont were used in this study: (1) HX6000 and (2) HX8000. HX6000 is a semicrystalline TLCP with no discernible glass transition temperature, two melting endotherms (one at 275.5°C and the second at 331.9°C), and a density of 1.38 g/cm^3. A melt temperature of at least 350°C is usually needed for processing. HX8000 is a semicrystalline TLCP with a glass transition temperature of 110°C, two melting endotherms (one at 228.9°C and the second at 271.8°C), and a density of 1.38 g/cm^3. To process this TLCP, a melt temperature of at least 290°C is typically needed. Both of these materials are believed to be composed of various ratios of terephthalic acid, 4-hydroxybenzoic acid (HBA), hydroquinone, and hydroquinone derivatives, with HX6000 containing higher levels of HBA [3,23–31].

2.2. Specimen preparation

Before processing, all pellets were dried in a vacuum oven at 110°C for at least 24 h. They were then dry blended at the desired weight fractions and melt blended by injection molding using an Arburg Allrounder 221-55-250 injection molding machine. The mold used to produce the samples was a 75 mm × 80 mm × 1.6 mm film-gated plaque mold. The injection molder had a 22 mm diameter screw with a check ring non-return valve and a nozzle tip with a 2 mm orifice diameter. The screw speed used was 200 rev/min, with the injection pressure held at approximately 5 MPa and the holding pressure set at about 10 MPa. The residence time in the injection molder was 1–2 min, with over 30 s spent in the metering zone and reservoir.

The zone temperatures were the same regardless of the material being injection molded. Progressing from the solids conveying zone to the nozzle, the temperatures were: zone 1, 310°C; zone 2, 350°C; zone 3, 360°C; zone 4, 310°C. Note that for all plaques, the mold was kept at room temperature.

2.3. Dynamic rheological testing

Rheological measurements were conducted using a Rheometrics RMS-800 with 25 mm diameter parallel plate tooling. Dynamic oscillatory measurements were carried out using 5% strain and a gap of 1.0 mm. The test specimens were circular disks cut from the injection molded plaques. These were dried in a vacuum oven at 110°C for at least 24 h prior to testing. Each sample was brought to the starting test temperature and held at that temperature until thermal equilibrium was established between the tooling and the melt. This generally took 3–5 min. The temperature was measured using a thermocouple located in the center of the bottom plate. For the duration of the tests, each sample was exposed to a continuous nitrogen atmosphere.

To monitor for thermal stability, the complex viscosity ($|\eta^*|$) of the melt was repeatedly measured over time. These tests, called rheological time sweeps, were conducted using an angular frequency (ω) of 10 rad/s and a run time of 30 min. Care was taken to note the condition of the melt at the conclusion of each test, checking for offgassing and discoloration. Offgassing was characterized by the formation of bubbles in the melt during the testing.

To examine the rheology of supercooled TLCPs, the $|\eta^*|$ of the melt was measured as the TLCP was cooled. An angular frequency of 10 rad/s was used in each test. The specimen was brought to the starting test temperature, then cooled at a constant rate. The cooling rates used usually ranged from 2.3°C/min to 15.0°C/min. The test was stopped once the torque exceeded 500 g·cm. Typically, a starting melt temperature of 360°C was used.

For the dynamic mechanical analysis, strips were cut in the machine direction from the injection molded plaques and the cut surfaces sanded. They were tested in air, using an angular frequency of 10 rad/s, a percent strain of 0.1, and a heating rate of 2.5°C/min.

2.4. Differential scanning calorimetry testing

A Perkin-Elmer DSC 7 was used for the differential scanning calorimetry testing, with a constant purge of argon bathing the sample. This is a highly accurate instrument, with an energy sensitivity of ± 0.01 mW, heating and cooling rate control of ± 0.05°C/min, and a temperature accuracy of ± 0.1°C [32,33].

The instrument was calibrated using indium and zinc standards. To account for any lag due to different heating and cooling rates, indium calibration was carried out at various heating rates. The offsets in measured transition temperatures for indium were then used to correct the experimentally recorded temperatures.

Because the injection molded plaques were too thick for use in DSC testing, an additional step was needed to make thin films from the plaques. This step consisted of taking one plaque of each TLCP and pressing it into a thin film using a Pasadena Hydraulic press set at 350°C. The plaques were placed between Kapton sheets, then inserted between the press platens for 30 s without applying pressure. After the 30 s had elapsed, 6.90 MPa of pressure was applied for an additional 30 s. The film was subsequently removed from the press and immediately quenched in an ice bath. From these films, a punch was used to remove samples having a consistent circular disc-shaped geometry. The test samples ranged in weight from 20 to 25 mg, as determined using a Mettler ME30 microbalance. This balance has a range of 0–30 mg, with an error of ± 0.030 mg. Before testing, the material was dried in a vacuum oven at 110°C for at least 24 h.

To determine the thermal stability of the material, the DSC samples were cyclically exposed to 360°C for increasingly long times. First, the sample was rapidly taken to 360°C, allowed to establish thermal equilibrium, then cooled at a fixed rate. Each cooling rate used in the DSC tests matched the fastest cooling rate obtained in the rheological cooling scans of that material. After cooling, it was reheated at a rate of 20.0°C/min to 360°C, kept at that temperature for 15 min, and then cooled again. This procedure was repeated until the total exposure time to 360°C was 60 min. The cooling scans provided the onset of crystallization temperature and the peak crystallization temperature while the heating scans provided the peak melting temperature and the enthalpy of melting. It has been established in studies of other polymers that measuring changes in these quantities was an extremely accurate method for determining thermal stability [34,35]. In particular, changes in these quantities occurred when the polymers underwent chemical reactions in the melt.

2.5. Morphology

The morphology of the blends was examined using a Stereoscan S200 scanning electron microscope with an accelerating voltage of 20 kV. To prepare the three samples, they were heated in the Rheometrics RMS-800 at 360°C for 5, 15, and 25 min, respectively. They were then attached to mounting stubs and coated with a layer of gold using a Bal-Tec SCD 005 sputter coater to enhance conductivity.

3. Results and discussion

To examine the effect of blend composition on crystallization, rheological cooling scans were performed. This was done for both the neat TLCPs as well as for blends containing 25/75, 50/50, and 75/25 wt% of the two components. To help interpret the rheological results, the term ‘solidification temperature’ is defined as the temperature at which the magnitude of the complex viscosity ($|\eta^*|$) begins to dramatically rise with additional cooling. In cases where a crystalline melting point is evident, this increase in viscosity is expected to be due to crystallization. Experimentally, the solidification temperature was arbitrarily determined by finding the temperature at which the viscosity increased by 20% per °C of cooling.

To determine the effect of composition on the solidification temperature of the HX6000/HX8000 blends,

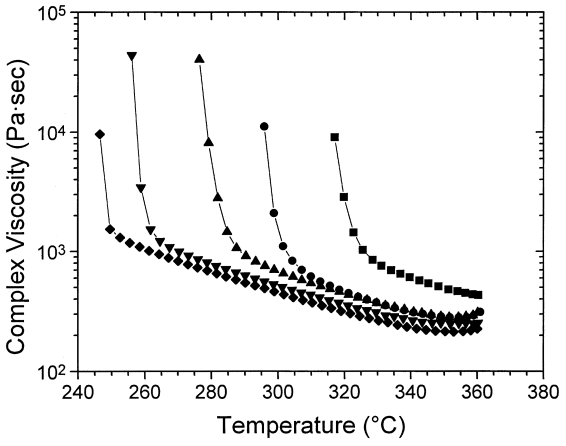

Fig. 1. The complex viscosity ($|\eta^*|$) versus temperature of the neat TLCPs and HX6000/HX8000 blends, using a cooling rate of 2.3°C/min (± 0.1°C/min). ■, neat HX6000; ●, HX6000/HX8000 (75/25 wt%; ▲, HX6000/HX8000 (50/50 wt%; ▼, HX6000/HX8000 (25/75 wt%; ◆, neat HX8000.

measurements of $|\eta^*|$ were made as the melt was cooled. As shown in Fig. 1, composition significantly influenced the solidification temperatures of the blends. For example, neat HX6000 could only be cooled to 322.7°C before $|\eta^*|$ climbed rapidly, while the 50/50 wt% blend of HX6000/HX8000 reached a temperature of 281.9°C. Similar changes in viscosity were seen for the other blends of HX6000 and HX8000, with the addition of larger amounts of HX8000 allowing the melt to be cooled to lower temperatures. Because HX6000 possessed a solidification temperature of 322.7°C and HX8000 had a solidification temperature of 252.5°C, this meant that it was possible to tailor the supercooling behavior of these melt blends over a 70°C range by simply changing the composition.

Having shown that the solidification temperature could be changed by varying the composition of the blend, it needed to be determined if cooling rate would have an effect on the solidification temperature. This was done by performing tests at three additional cooling rates of approximately 4.5°C/min, 8.3°C/min, and 15.1°C/min on the TLCP/TLCP blends. The results of the tests revealed that cooling at a faster rate allowed the polymer to reach a lower temperature before significant solidification began (Table 1). Also, it appeared that even lower solidification could be reached if the melt was cooled at a faster rate, such as the estimated 1000°C/min found in fiber spinning [36]. Of course, these results are expected as crystallization kinetics are very slow in these temperature regimes.

The effect of composition on the solidification temperature at the higher cooling rates was also examined. It was found that regardless of the cooling rate used, the addition of more HX8000 to the HX6000/HX8000 blend allowed the melt to be brought to a lower temperature before the complex viscosity began to rise dramatically (Table 1). One interesting point was that at each cooling rate, applying a linear fit to the plot of composition versus solidification temperature gave a correlation coefficient (r^2) of about 0.99. This indicates that if the solidification temperature is known for the two neat TLCPs at any cooling rate, a linear interpolation based on composition will provide an accurate prediction of the solidification temperature for any HX6000/HX8000 blend.

Because the rheological tests showed that HX6000 was more sensitive to cooling rate than HX8000, the effect of blend composition on this sensitivity was investigated. The results shown in Table 1 demonstrate that composition did have an effect. For HX8000, there was a 9.2°C difference in solidification temperatures when a cooling rate of 2.4°C/min was used rather than a rate of 16.3°C/min. As the cooling rate increased from 2.4°C/min to 14.9°C/min for the 50/50 wt% blend, the difference between the solidification temperatures rose to 10.1°C. Furthermore, the neat HX6000 displayed a 15.3°C reduction in solidification temperature as the cooling rate rose from 2.3 to 14.3°C/min. Hence, the sensitivity of the blends to cooling rate was between those of the neat TLCPs, with higher concentrations of HX6000 making the effect of cooling rate more pronounced.

To complement the rheological tests, DSC cooling scans were performed while varying the cooling rate and blend composition. From this examination, it was clear that blend composition had a significant effect on the peak crystallization temperature, with the crystallization exotherm shifted to lower temperatures as the concentration of HX8000 was increased (Table 2). Investigating the effect of composition on the peak crystallization temperatures of the TLCPs showed that a linear relationship existed, with a correlation coefficient of 0.999. Note that this same behavior was observed in the rheological cooling tests, showing that the monotonic relationship between solidification temperature and composition observed in the rheological cooling curves was closely reproduced in the DSC cooling scans.

The effect of cooling rate on the onset of crystallization temperature of the 50/50 wt% blend was investigated and compared with the neat TLCPs. As presented in Table 3, faster cooling rates produced lower onset of crystallization temperatures, qualitatively matching the relationship between solidification temperature and cooling rate found in the rheological testing. Furthermore, the onset of

Table 1
The effect of blend composition and cooling rate on the solidification temperatures of HX6000/HX8000[a]

Approx. cooling rate (°C/min)	Solidification temperature (°C)					Correlation coefficient (r^2)[b]
	Composition of HX6000/HX8000 blends (wt%/wt%)					
	100/0	75/25	50/50	25/75	0/100	
2.3	322.7 (2.3)	301.5 (2.2)	284.7 (2.4)	261.7 (2.4)	249.5 (2.4)	0.993
4.5	315.7 (4.4)	303.1 (4.4)	281.7 (4.5)	260.3 (4.4)	245.8 (4.6)	0.991
8.3	310.5 (8.1)	299.5 (8.1)	275.3 (8.3)	259.2 (8.5)	242.3 (8.6)	0.991
15.1	307.4 (14.3)	293.0 (14.7)	271.8 (14.9)	257.5 (15.5)	240.1 (16.3)	0.997

[a] Values in parentheses are the experimental cooling rates (°C/min).
[b] Correlation coefficient is based on a linear best fit to the data.

Table 2
The effect of blend composition and cooling rate on the peak crystallization temperatures of HX6000/HX8000[a]

Approx. cooling rate (°C/min)	Peak crystallization temperature (°C)				
	Composition of HX6000/HX8000 blends (wt%/wt%)				
	100/0	75/25[b]	50/50	25/75[b]	0/100
2.3	308.18	***	274.62	***	238.28
	(2.3)		(2.4)		(2.4)
4.5	303.04	***	268.23	***	234.01
	(4.4)		(4.5)		(4.6)
8.3	294.76	***	264.86	***	230.72
	(8.1)		(8.3)		(8.6)
15.1	289.71	274.11	258.78	240.78	226.46
	(14.3)	(14.7)	(14.9)	(15.5)	(16.3)

[a] Values in parentheses are the experimental cooling rates (°C/min).
[b] Only the fastest cooling rate was used in testing the blends with compositions of 75/25 wt% and 25/75 wt% HX6000/HX8000. Note that the starting temperature for all tests was 360°C.

crystallization temperature did not appear to level off in the range of cooling rates examined, suggesting that higher cooling rates may lower the crystallization temperature even further. From this it can be concluded that cooling rate had a similar effect on both the solidification temperature and the onset of crystallization temperature.

However, although the trends in the DSC and rheological cooling tests were similar, they did not match one another precisely. As illustrated in Fig. 2, it was clear that the rise in $|\eta^*|$ did not coincide with the onset of crystallization, with the complex viscosity consistently increasing before any change in the melt was detected by differential scanning calorimetry. Specifically, the complex viscosity rose to well over 10 000 Pa·s before any changes were detected in the DSC scans. This result is important because it helps demonstrate that differential scanning calorimetry can not be used to quantify how low a temperature the melt can be cooled to before it is no longer deformable. Thus, rheological cooling scans rather than DSC cooling scans should be used to establish processing guidelines for these supercooled melts.

There are several possible reasons for the difference between the rheological and DSC cooling tests. One possibility is that the strain applied during the dynamic oscillatory tests caused the melt to begin solidifying. In particular, it has been shown in isothermal crystallization studies of polyethylene that strain can influence when the melt begins crystallizing [37]. A second possibility is that the difference is due to the fact that DSC measures changes in energy flow while the rheological testing measures changes in deformability and structure. Rheological tests are very sensitive to changes in structure, so it is possible that the initial crystallization is easily measured rheologically while remaining within the experimental noise of the DSC measurements. A third potential reason for this behavior is that a radial temperature gradient exists in the rheological test samples. The temperature is taken from the center of the parallel plate fixtures, while the rheological response of the melt is dominated by the behavior of the melt at the edge of the parallel plate fixtures. If the melt is cooler at the edge of the parallel plates, the complex viscosity would begin to rise at a higher apparent temperature. Also, it is possible that the results

Table 3
The effect of blend composition and cooling rate on the onset of crystallization temperatures of HX6000/HX8000[a]

Approx. cooling rate (°C/min)	Onset of crystallization temperature (°C)				
	Composition of HX6000/HX8000 blends (wt%/wt%)				
	100/0	75/25[b]	50/50	25/75[b]	0/100
2.3	313.10	***	279.30	***	241.44
	(2.3)		(2.4)		(2.4)
4.5	308.97	***	274.41	***	236.67
	(4.4)		(4.5)		(4.6)
8.3	301.54	***	270.70	***	233.48
	(8.1)		(8.3)		(8.6)
15.1	296.41	280.09	264.75	248.94	229.49
	(14.3)	(14.7)	(14.9)	(15.5)	(16.3)

[a] Values in parentheses are the experimental cooling rates (°C/min).
[b] Only the fastest cooling rate was used in testing the blends with compositions of 75/25 wt% and 25/75 wt% HX6000/HX8000. Note that the starting temperature for all tests was 360°C.

from the two tests differed because something unique about the crystallization process may exist which we do not understand at this time.

Tests were conducted to determine if strain affects the time at which the melt solidifies. HX6000/HX8000 (50/50 wt%) blends were cooled at a rate of 2.4°C/min (± 0.1°C/min) using four different strains (1%, 5%, 10%, and 20%). It was found that strain did not have a significant effect on the time at which the complex viscosity began to rise. Therefore, the melt was not influenced by the strain used in the rheological cooling scans.

It is likely that a small temperature gradient does exist in the rheological test specimens though, which could influence solidification behavior. In cooling scans performed using a cooling rate of 2.4°C/min, it was found that the oven temperature was 3–4°C cooler than the temperature measured with the parallel plate thermocouple. Note that the oven thermocouple was mounted close to the insulated wall, near where the cooling nitrogen initially enters the oven. In addition, Mora and Macosko [38,39] have determined that even at steady state, temperature gradients exist in the polymer melt. They also determined that the temperature difference between the center and edge of the sample increased during nonisothermal tests. Therefore, it is possible that temperature gradients within the polymer melt may account for the discrepancy between the rheological and DSC cooling scans, with the parallel plate edges being slightly cooler than the center of the parallel plate.

Still, it should be recognized that to determine the precise cause or causes for this difference requires a comprehensive study. Specifically, rheo-optical techniques would be needed to monitor changes in structure as the melt was cooled. This would require specialized tooling to allow in situ measurements to be made. Also, a series of accurate thermocouples or platinum resistance thermometers would need to be mounted within the gas convection oven and on the parallel plate fixtures to precisely determine the temperature gradients which exist during testing. Because this work is focused on the crystallization behavior of the TLCP/TLCP blends and how it compares with the neat TLCPs, addressing these concerns is beyond the scope of this study.

Heating samples from room temperature, the effects that composition had on the dynamic mechanical properties of these blends were investigated as a function of temperature. First, the effect of composition on the change in modulus versus temperature was examined. From this it was found that adding HX6000 to HX8000 allowed the TLCP to retain its stiffness at higher temperatures. For HX8000, the storage modulus began to drop dramatically at around 220°C, while the HX6000/HX8000 (50/50 wt%) blend retained a high modulus to about 240°C and neat HX6000 did not exhibit a decline in storage modulus until the temperature reached approximately 260°C. Similar trends were found for the loss moduli of the blends, with the 50/50 wt% blend showing a decline in loss modulus at a temperature roughly halfway between those found for neat HX6000 and neat HX8000. These results demonstrate that the temperature at which the modulus falls dramatically can be controlled by varying the blend composition.

Second, the effect of composition on the storage and loss moduli was studied as the specimens were heated. At temperatures past 100°C, the storage and loss moduli were increased slightly as the concentration of HX6000 increased (Figs 3 and 4). For example, at 175°C, the storage modulus of HX8000 was 2.35×10^8 Pa, while for HX6000/HX8000 (50/50 wt%) it was 3.80×10^8 Pa and for neat HX6000 it was 4.70×10^8 Pa. This means that blend composition can be used as a means to control the stiffness of the samples. Note that this increase in stiffness was believed to be due to the inherent higher stiffness of HX6000 and not due to the blends possessing a higher degree of crystallinity. In particular, DSC scans showed that the enthalpies of melting were greater for the neat TLCPs than they were for the blends, suggesting the blends were less crystalline (Table 4).

To complement the DMTA tests, DSC heating scans were performed to show how changing the blend composition

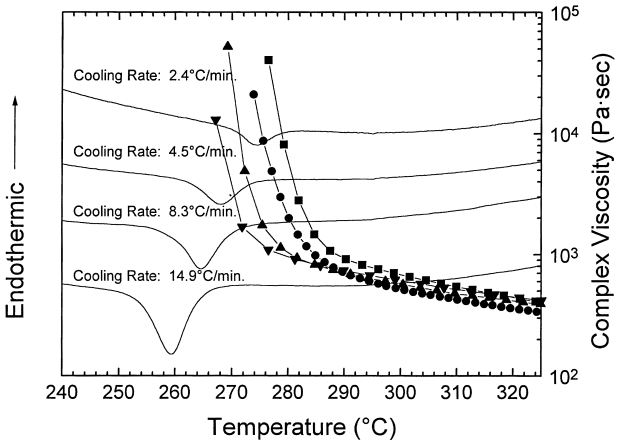

Fig. 2. Rheological and DSC cooling scans for HX6000/HX8000 (50/50 wt%) blends. Complex viscosity at the various cooling rates: ■, 2.4°C/min; ●, 4.5°C/min; ▲, 8.3°C/min; ▼, 14.9°C/min.

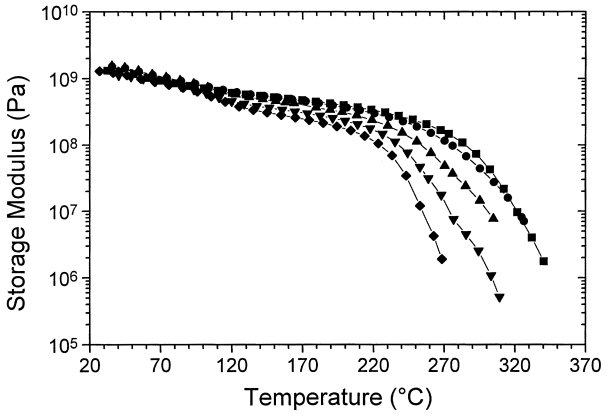

Fig. 3. Storage modulus (G') versus temperature of the neat TLCPs and HX6000/HX8000 blends, using a heating rate of 2.5°C/min (± 0.1°C/min). ■, neat HX6000; ●, HX6000/HX8000 (75/25 wt%; ▲, HX6000/HX8000 (50/50 wt%); ▼, HX6000/HX8000 (25/75 wt%); ◆, neat HX8000.

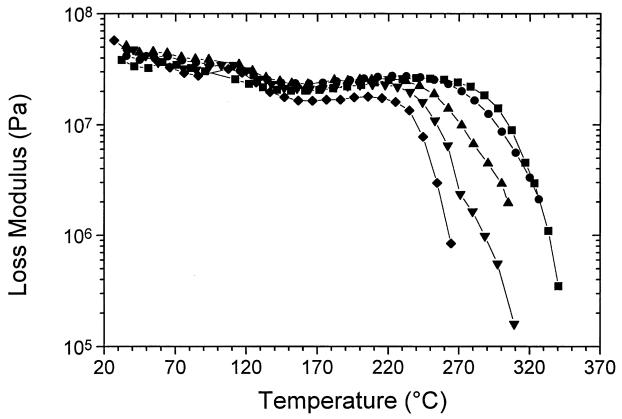

Fig. 4. Loss modulus (G'') versus temperature of the neat TLCPs and HX6000/HX8000 blends, using a heating rate of 2.5°C/min (± 0.1°C/min). ■, neat HX6000; ●, HX6000/HX8000 (75/25 wt%); ▲, HX6000/HX8000 (50/50 wt%); ▼, HX6000/HX8000 (25/75 wt%); ◆, neat HX8000.

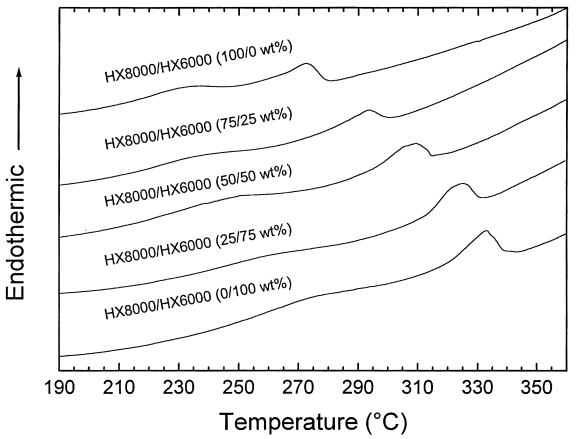

Fig. 5. DSC heating scans of the neat TLCPs and HX6000/HX8000 blends, using a heating rate of 20.0°C/min.

affected the peak melting endotherms. Consistently, the blends possessed two melting endotherms, with both shifting to lower temperatures as the concentration of HX8000 was increased (Fig. 5). This is very intriguing behavior because most polymer blends display separate melting endotherms for each component, so it would be expected that the HX6000/HX8000 blends would display four endotherms, not two. This complements the dynamic mechanical analysis shown in Figs 3 and 4 because in those tests, the blends did not exhibit separate drops in storage and loss moduli due to each component softening. Rather, the blend softened at a temperature that was a function of the blend composition, like a homogeneous material. Therefore, combining the DSC heating scan results with the previously presented rheological, dynamic mechanical, and differential scanning calorimetric results, it must be concluded that either (1) the two TLCPs are miscible and co-crystallize or (2) they underwent a reaction (such as ester interchange) during the processing step to produce a new TLCP of intermediate composition.

Before performing any experimental work, it needed to be ascertained if appreciable ester interchange could occur at the processing temperatures used for these TLCP/TLCP blends. In particular, it should be noted that several research groups have demonstrated that under the proper conditions, TLCPs can undergo ester interchange reactions even without the addition of a catalyst [15,40–44]. To calculate the amount of time for ester interchange to take place, an Arrhenius rate of reaction expression determined by MacDonald et al. [45] for a TLCP (number average molecular weight 71 400) was applied to the HX6000/HX8000 blends. Specifically, MacDonald and coworkers used small-angle neutron scattering to study the transesterification kinetics of a TLCP composed of hydroquinone (HQ), isoterephthalic acid (IA), and 4-hydroxybenzoic acid (HBA) (32/32/36 mol%), a composition similar to those cited for TLCPs manufactured by DuPont [24–31]. They found that although the rate of reaction for this TLCP was slower than had been reported for PET [46], at 330°C the time for the approach to equilibrium monomer distribution was 30 min. Furthermore, when the Arrhenius rate expression was applied to the ester interchange reactions of blends of 75/25 and 30/70 mol% copoly(HBA/HNA) reported by McCullagh et al. [15], the predicted time of 60 min for complete randomization matched the experimental observations determined through X-ray diffraction. The fact that the rate expression predicted the randomization time for copolyesters of HBA and HNA as well as the original HQ/IA/HBA TLCP for which it was developed, suggested that it may be generally applicable to many wholly aromatic main-chain TLCPs. Additionally, because the composition of HQ/IA/HBA (32/32/36 mol%) was similar to that reported for the TLCPs produced by DuPont, it was likely that the Arrhenius rate expression would provide a good qualitative estimate of

Table 4
The effect of composition on the enthalpy of melting and peak melting temperatures of blends of HX6000/HX8000

HX6000/HX8000 (wt%/wt%)	Enthalpy of melting (J/g)	First peak melting temperature (°C)	Second peak melting temperature (°C)
100/0	2.45	275.52	331.92
75/25	1.52	258.12	322.59
50/50	2.19	249.19	307.52
25/75	1.46	233.99	292.63
0/100	2.49	228.94	271.79

Note: The heating rate used was 20.0°C/min.

the time needed for complete randomization in the HX6000/HX8000 blends. Assuming this was the case, at 360°C it was calculated that the transesterification reaction would randomize the mesogenic units in the polymer chains in only 5.9 min. Considering that the residence time in the injection molder was 1–2 min, with over 30 s spent in the metering zone and reservoir, this calculation strongly suggests that significant ester interchange would have occurred when the blends were injection molded.

To attempt to experimentally confirm this prediction, X-ray diffractometry was performed. This served to determine if a difference in *d*-spacings existed between HX6000 and HX8000, which could then be used to prove that ester interchange between the two TLCPs had taken place. Unfortunately, the X-ray diffractometry scans of the neat HX6000 and HX8000 specimens revealed no difference in the *d*-spacings of the observed maxima. This meant that although McCullagh and coworkers [15] showed that X-ray diffractometry was a powerful method of discerning transesterification reactions in blends of 75/25 and 30/70 mol% copoly(HBA/HNA), it was not able to provide any further insight into the nature of the TLCP/TLCP blends used in this study.

However, other experimental evidence indicated that chemical reactions had occurred in the melt, although they could not be proven to be transesterification reactions. Measuring the complex viscosity over time showed that neither the neat TLCPs nor the TLCP/TLCP blends were stable at 360°C, despite being tested in a nitrogen atmosphere (Fig. 6). Consistently, the complex viscosity first dropped and then began to increase, usually after 10–25 min. Also, rheological tests conducted at higher temperatures showed that the increase in viscosity over time occurred sooner and became more pronounced as the temperature was increased [22]. Examining the rheological specimens after the 30 min testing period, it was noticed that they were slightly discolored and contained bubbles, indicating that volatile products were released. To illustrate the formation of bubbles in the melt over time, scanning electron micrographs of samples exposed to 360°C for 5, 15, and 25 min were taken (Fig. 7). These micrographs clearly show that as the exposure time to 360°C was increased, the number of bubbles present also increased. Summarizing, the formation of bubbles, discoloration, and change in viscosity over time

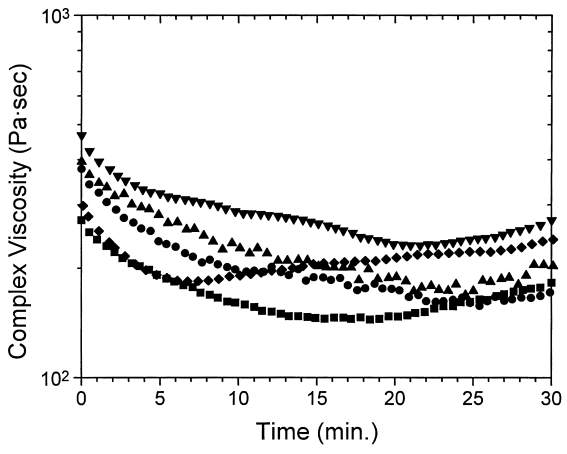

Fig. 6. Complex viscosity ($|\eta^*|$) versus time at 360°C. ■, neat HX6000; ●, HX6000/HX8000 (75/25 wt%); ▲, HX6000/HX8000 (50/50 wt%); ▼, HX6000/HX8000 (25/75 wt%); ◆, neat HX8000.

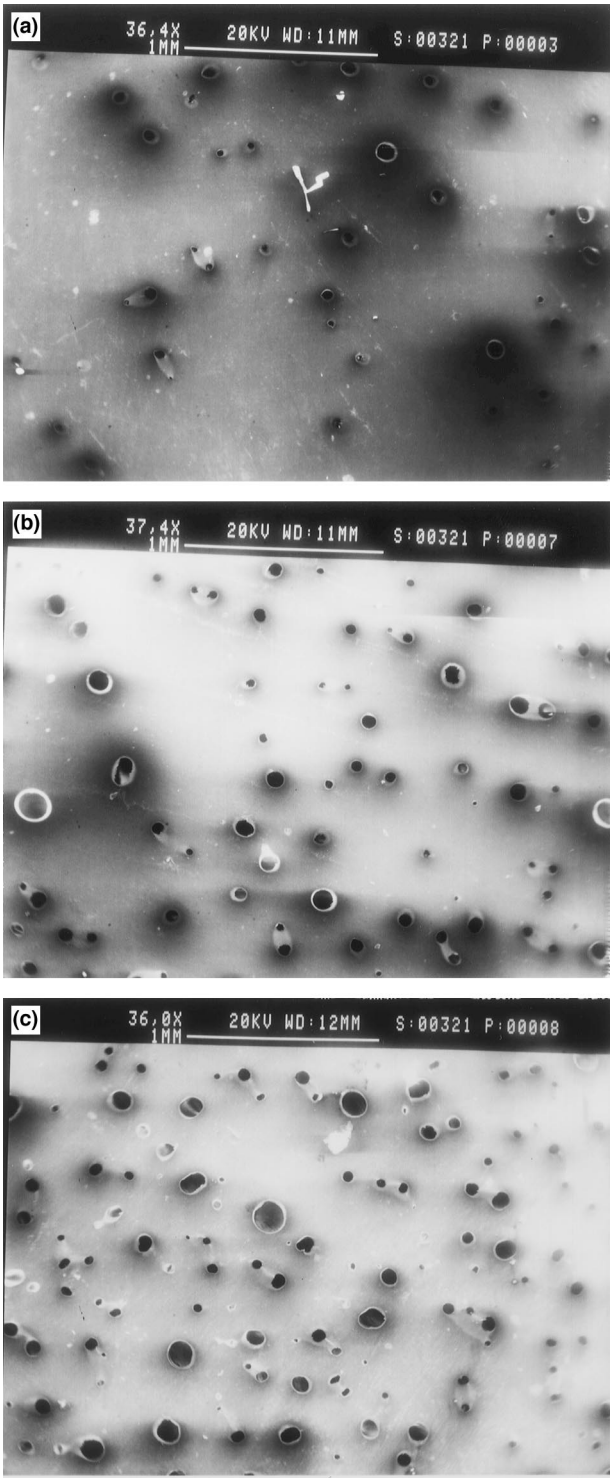

Fig. 7. Scanning electron micrographs of HX6000/HX8000 (50/50 wt%) exposed to 360°C for different exposure times: (a) 5 min; (b) 15 min; (c) 25 min.

were all consistent with reactions occurring in the melt. Moreover, because HX6000 and HX8000 are believed to have similar compositions, it would be expected that these two TLCPs would react both with themselves as well as with one another.

To determine the effect that exposure to 360°C would have on the crystallization and melting behavior of these polymers, repeated heating and cooling DSC scans were performed on HX6000, HX8000/HX6000 (50/50 wt%), and HX8000, incrementally keeping the polymer at 360°C for longer times. These revealed that increased exposure to 360°C shifted the peak crystallization temperature and the onset of crystallization temperature of both the neat TLCPs and the blend to lower values, which was what would be expected if the molecular weight was building (Table 5). Also, during the heating scans, longer exposure to 360°C lowered the enthalpy of melting of these materials, which was consistent with a system experiencing an increase in molecular weight. Note that it has been shown in a few studies of TLCPs that an increase in molecular weight can occur during transesterification reactions in the melt [35,41], so this may have been the cause of the apparent rise in molecular weight for the neat TLCPs as well as the TLCP/TLCP blends. However, the possibility that other reactions occurred to produce these results can not be discounted.

Motivated by the formation of bubbles in the rheological test specimens, the DSC samples were weighed before and after testing. When this was done, it was found that each specimen had a slightly lower mass at the end of the DSC scans than it possessed at the beginning. For the HX6000 sample, the initial mass was 23.810 mg and the final mass was 23.652 mg, a drop of 0.66%. Almost identical results were measured for the HX6000/HX8000 (50/50 wt%) sample, with a mass of 23.809 mg at the beginning of the test but only 23.650 mg after the test was concluded. Meanwhile, the HX8000 sample had a drop in mass of 0.69%, starting at 23.137 mg and having a final mass of 22.978 mg. These data further lend credence to the idea that the melt underwent reactions, which could have served to produce a new polymer of intermediate composition when the HX6000 and HX8000 were blended together.

4. Conclusions

In this study, it was shown that by blending HX6000 and HX8000 together it was possible to vary the melting temperature over a 60°C temperature range, with the crystallization temperature of the blends rising linearly as the weight fraction of HX6000 was increased. Through DSC and rheological testing it was determined that both cooling rate and blend composition had an effect on the crystallization behavior of these blends. Cooling the melt faster allowed the blends to reach lower temperatures before

Table 5
The effect of exposure to 360°C on the calorimetric properties of HX6000, HX6000/HX8000 (50/50 wt%), and HX8000

Exposure time to 360°C (min)	Peak crystallization temp. (°C)	Onset of crystallization temperature (°C)	Peak melting temperature[a] (°C)	Enthalpy of melting (J/g)
Neat HX6000				
0	289.15	294.94	333.03	2.21
15	287.88	290.59	332.40	1.52
30	287.22	289.91	332.00	1.53
45	286.56	289.35	332.70	1.20
60	285.96	288.77		
HX6000/HX8000 (50/50 wt%)				
0	259.89	265.62	308.12	2.14
15	255.50	260.40	304.62	2.17
30	254.36	258.67	303.62	2.02
45	253.68	257.67	303.28	1.94
60	253.17	256.93		
Neat HX8000				
0	226.30	229.05	272.30	2.49
15	224.50	227.61	272.40	2.14
30	223.68	226.95	272.70	1.76
45	223.04	226.50	270.70	1.55
60	222.46	225.70		

[a]Peak melting temperature for the second melting endotherm.

Note: the cooling rates used to determine the peak crystallization and onset of crystallization temperatures were 14.3°C/min for HX6000, 14.9°C/min for HX6000/HX8000 (50/50 wt%), and 16.3°C/min for HX8000. The heating rate of 20.0°C/min was used in all tests to determine the peak melting temperature and enthalpy of melting.

crystallization occurred, while increasing the concentration of HX6000 in the blends caused the crystallization behavior to become more sensitive to cooling rate. Comparing the DSC and rheological cooling test results, the complex viscosity consistently rose before the onset of crystallization was detected in the DSC.

Although calculations suggested that the two TLCPs could have undergone ester interchange reactions as they were injection molded, this was not proven conclusively. Still, the rheological and differential scanning calorimetric test results indicated that an undetermined reaction had occurred when the melt was taken to 360°C, increasing the molecular weight of the polymer over time. It is speculated that this reaction helped to create the crystallization and dynamic mechanical thermal analysis behavior of these materials.

Acknowledgements

The authors gratefully recognize the support from the Army Research Office (Grant #: DAAH04-94-G-0171). Also, we offer our appreciation to DuPont for donating the thermotropic liquid crystalline polymers used in accomplishing this study.

References

[1] Calundann GW, Jaffe M. Proc of the Robert A Welch Foundation Conferences on Chemical Research 1983;26:247.
[2] Luise RR. In Salamone JC, editor. Polymeric materials encyclopedia (liquid crystalline polymers (heat-strengthened, thermotropic)). Boca Raton, FL: CRC Press, 1996.
[3] Figuly GD. In: Salamone JC, editor. Polymeric materials encyclopedia (liquid crystalline polymers (thermotropic polyesters)). Boca Raton, FL: CRC Press, 1996.
[4] Roggero A. In: La Mantia FP, editor. Thermotropic liquid crystal polymer blends, chap. 6. Lancaster, PA: Technomic Publ. Co., 1993.
[5] Brown CS, Alder PT. In: Folkes MJ, Hope PS, editors. Polymer blends and alloys. London: Chapman and Hall, 1993.
[6] Ramanathan R, Done DS, Baird DG. SPE ANTEC ’89 Tech Pap 1989;35:1716.
[7] Isayev AI. SPE ANTEC ’91 Tech Pap 1989;37:908.
[8] Akhtar S, Isayev AI. Polym Eng Sci 1993;33:32.
[9] Ding R, Isayev AI. J Thermoplastic Comp Mater 1995;8:208.
[10] De Meuse MT, Jaffe M. Mol Cryst Liq Cryst Inc Nonlin Opt 1988;157:535.
[11] De Meuse MT, Jaffe M. In: Weiss RA, Ober CK, editors. Liquid crystalline polymers. ACS Symp. Ser. No. 435. Washington, DC: ACS, 1990.
[12] De Meuse MT, Jaffe M. SPE ANTEC ’91 Tech Pap 1991;37:905.
[13] Kenig S, De Meuse MT, Jaffe M. Polym Adv Tech 1991;2:25.
[14] Done D, Baird DG. Polym Eng Sci 1990;30:989.
[15] McCullagh CM, Blackwell J, Jamieson AM. Macromolecules 1994;27:2996.
[16] Baird DG, Sukhadia AM. US Patent 5,225,488, 1993 (Virginia Polytechnic Institute and State University).
[17] Sukhadia AM, Datta A, Baird DG. Int Polym Proc 1992;VII:218.
[18] Sabol EA, Handlos AA, Baird DG. Polym Comp 1995;16 (4):330.
[19] Robertson CG, de Souza JP, Baird DG. In: Isayev AI, Kyu T, Cheng SZD. Liquid–crystalline polymer systems: technological advances. Washington, DC: ACS Books, 1996.
[20] Machiels AGC, Denys KFJ, Van Dam J, Posthuma De Boer AA. Polym Eng Sci 1996;36:2450.
[21] Krishnaswamy RK, Baird DG. Polym Compos 1997;18:526.
[22] McLeod MA. PhD dissertation, Virginia Polytechnic Institute and State University, 1997.
[23] Magagnini P. In: La Mantia FP, editor. Thermotropic liquid crystalline polymer blends. Lancaster, PA: Technomic, 1993.
[24] Avakian P, Coburn JC, Connolly MS, Sauer BB. Polymer 1996;37:3843.
[25] Kleinschuster JJ. US Patent 3,991,014, 1976 (DuPont).
[26] Irwin RS. US Patent 4,487,916, 1984 (DuPont).
[27] Irwin RS. US Patent 4,496,712, 1985 (DuPont).
[28] Irwin RS. US Patent 4,499,259, 1985 (DuPont).
[29] Connolly MS. US Patent 4,664,972, 1987 (DuPont).
[30] Samuels MR, Waggoner MG. US Patent 5,466,773, 1995 (DuPont).
[31] Samuels MR, Waggoner MG. US Patent 5,525,700, 1996 (DuPont).
[32] Perkin Elmer Product Literature. DSC 7 differential scanning calorimeter, Order No. L-1152C.
[33] Perkin Elmer Instrument Manual.
[46] Kugler J, Gilmer JW, Wiswe D, Zachmann HG, Hahn K, Fischer EW. Macromolecules 1987;20:1116.
[34] Jonas A, Legras R. Polymer 1991;32:2691.
[35] Porter RS, Wang L-H. Polymer 1992;33:2019.
[36] Robertson CG. Master’s thesis, Virginia Polytechnic Institute and State University, 1995.
[37] Young R, Baird DG. Unpublished data, 1998.
[38] Mora E, Macosko CW. Proc North Am Therm Anal Soc, 1991;20:506.
[39] Macosko CW. In: Rheology: principles, measurements, and applications. New York: VCH Publishers, 1994.
[40] Mühlebach A, Economy J, Johnson RD, Karis T, Lyerla J. Macromolecules 1990;23:1803.
[41] Economy J, Johnson RD, Lyerla JR, Mühlebach A. In: Weiss RA, Ober CK, editors. Liquid crystalline polymers. ACS Symp. Ser. No. 435. Washington, DC: ACS, 1990.
[42] Blackwell J, Schneider A-I, McCullagh CM. Mater Res Soc Symp Proc 1994;321:71.
[43] Li MH, Brûlet A, Keller P, Strazielle C, Cotton JP. Macromolecules 1993;26:119.
[44] Mehta R. Master’s thesis, Virginia Polytechnic Institute and State University, 1989.
[45] MacDonald WA, McLenaghan ADW, McLean G, Richards RW, King SM. Macromolecules 1991;24:6164.